Annexin A2 contributes to lung injury and fibrosis by augmenting factor Xa fibrogenic activity

Michael Schuliga[1,2,3], Jade Jaffar[4], Asres Berhan[1], Shenna Langenbach[1], Trudi Harris[1], David Waters[2,3], Peter VS Lee[5], Christopher Grainge[3,6], Glen Westall[4], Darryl Knight[2,3,7] & Alastair G Stewart[1]

[1]Lung Health Research Centre, Department of Pharmacology and Therapeutics, University of Melbourne, Parkville, Victoria, Australia.
[2]School of Biomedical Sciences and Pharmacy, University of Newcastle, Callaghan, New South Wales, Australia.
[3]Priority Research Centre for Healthy Lungs, Hunter Medical Research Institute, New Lambton Heights, New South Wales, Australia.
[4]Allergy, Immunology and Respiratory Medicine, Alfred Hospital, Prahran, Victoria, Australia.
[5]Dept. Mechanical Engineering, University of Melbourne, Parkville, Victoria, Australia.
[6]School of Medicine and Public Health, University of Newcastle, Callaghan, New South Wales, Australia.
[7]Department of Anesthesiology, Pharmacology and Therapeutics, University of British Columbia, Canada.

Correspondence Dr Michael Schuliga, School of Biomedical Sciences and Pharmacy, University of Newcastle, HMRI Building, New Lambton Heights, NSW 2305, Australia, email: Michael.Schuliga@newcastle.edu.au

Running head Annexin A2-dependent FXa actions in lung fibrosis

Abstract

In lung injury and disease, including idiopathic pulmonary fibrosis (IPF), extravascular factor X is converted into factor Xa (FXa), a coagulant protease with fibrogenic actions. Extracellular annexin A2 binds to FXa, augmenting activation of the protease activated receptor-1 (PAR-1). In this study, the contribution of annexin A2 in lung injury and fibrosis was investigated. Annexin A2 immunoreactivity was observed in regions of fibrosis, including associated with fibroblasts in lung tissue of IPF patients. Furthermore, annexin A2 was detected in the conditioned media and an EGTA membrane wash of human lung fibroblast (LF) cultures. Incubation with human plasma (5% v/v) or purified FXa (15-50 nM) evoked fibrogenic responses in LF cultures, with FXa increasing interleukin-6 (IL-6) production and cell number by 270% and 46% respectively (*P<0.05, n=5-8). The fibrogenic actions of plasma or FXa were attenuated by the selective FXa inhibitor apixaban (10 μM), or antibodies raised against annexin A2 or PAR-1 (2 μg/mL). FXa-stimulated LFs from IPF patients (n=6) produced twice as much IL-6 as controls (n=10) (*P<0.05), corresponding with increased levels of extracellular annexin A2. Annexin A2 gene deletion in mice reduced bleomycin-induced increases in bronchoalveolar lavage fluid (BALF) IL-6 levels and cell number (*P<0.05, n=4-12). Lung fibrogenic gene expression and dry weight were reduced by annexin A2 gene deletion but lung levels of collagen were not. Our data suggests that annexin A2 contributes to lung injury and fibrotic disease by mediating the fibrogenic actions of FXa. Extracellular annexin A2 is a potential target for the treatment of IPF.

Key words

Apixaban, extracellular-regulated kinase (ERK), idiopathic pulmonary fibrosis (IPF), interstitial lung disease, protease activated receptor-1 (PAR-1)

Introduction

Pulmonary fibrosis, characterized by excessive accumulation of fibroblasts and collagen in lung parenchymal tissue, occurs in interstitial lung disease (ILD). The progressive form of pulmonary fibrosis in IPF, the most common ILD, is particularly devastating, resulting in inexorable decline in lung function and death (3). Whilst of unknown etiology, IPF is considered to be initiated by persistent injuries to the alveolar epithelium (44). The subsequent injury-repair responses to alveolar injury in IPF and other fibrotic ILDs (*eg.*, chronic hypersensitivity pneumonitis) are highly dysregulated, resulting in the persistence of fibroblasts and collagen that scar the lung. Lung fibroblast cytokine production and proliferation, which can be initiated within hours of a lung injury, have a central role in pulmonary fibrosis (6).

Vascular leak in lung injury and disease leads to plasma extravasation into parenchymal tissue. Plasma-borne factor X (FX) and VII (FVII), combined with locally produced tissue factor (TF), transforms FX into the active serine protease, FXa (41). Locally produced FX may also contribute to the pool of interstitial FXa in lung injury and disease. FX(a) mRNA is detected in alveolar epithelial cells, macrophages and fibroblasts in fibrotic foci of lung tissue from IPF patients (43). Together, FXa and factor Va (FVa) activate thrombin, the protease which cleaves fibrinogen into fibrin. Independent of its role in fibrin formation, FXa has important lung fibrogenic actions involving protease-activated receptors (PARs), a G-protein-coupled receptor family (43). PAR-1 is a FXa, thrombin and plasmin receptor, which is activated by proteolysis of the N-terminus to reveal a tethered ligand (41). FXa also activates PAR-2 by proteolysis, but only when FXa is complexed with TF and FVII (4). Fibroblast PAR-1 expression is increased in fibrotic lung disease (31). Inhibiting PAR-1 expression or activation reduces pulmonary inflammation and fibrosis in mouse models of lung injury and disease (18, 43, 58). Furthermore, PAR-1 activation evokes increased lung fibroblast cytokine and collagen expression, as well as proliferation (5, 33, 35, 43).

Annexin A2 is a 36 kDa calcium-binding protein with pleiotropic functions, having both intracellular and extracellular roles (17). The pathological roles of annexin A2 in diseases such as acute promyelocytic leukemia (21) and pancreatic ductal adenocarcinoma (57) are attributable to its extracellular functions. The annexin A2 secreted from cells is found either as a monomer or complexed with S100A10 (p11) to form a soluble hetero-tetrameric complex (denoted AIIt) (17). Annexin A2 binds the proteases FXa or plasmin (4, 30), augmenting PAR-1 activation (39, 41, 49). This *'transducer'* role may be facilitated by annexin A2 binding to the cell surface non-specifically via calcium chelation (17) or specifically to integrins (27). As a consequence of its FXa-transducer role, extracellular annexin A2 is a potential drug target in the treatment of tissue remodeling including fibrosis in disease.

In this study, we provide evidence that supports a role of extracellular annexin A2 in lung injury and fibrosis. Here, we show annexin A2 is associated with regions of fibrosis in IPF lung and that it augments FXa-stimulated lung fibroblast cytokine production and proliferation. Furthermore, annexin A2 gene deletion attenuated inflammation and features of fibrosis including lung fibrogenic gene expression and increased dry weight, but not lung collagen, in bleomycin-induced lung injury.

Methods

Cell culture

Lung fibroblast (LF) cell cultures were established as described previously (42) using lung tissue resections from patients or donors at the Alfred Hospital (Prahran, Melbourne, Australia) under ethical approval from the University of Melbourne (HREC980168X) and Alfred Hospitals (#336/13). Additional LF cultures were established from tissue of patients at the John Hunter Hospital (New Lambton Heights, Newcastle, Australia) under ethical approval from the Hospital (H-2016-0325). Depending on the status of the patients or donors, cultures were classified as either IPF or control (Ctrl, no evidence of ILD). Fibroblasts from control donors, between passages 4-11, were used in all experiments unless stated otherwise. Human embryonic MRC5 LFs were used, between passages 16-25, for selected experiments with human plasma of healthy adult volunteers. Cells were seeded onto 6, 24 or 96 well plates (2×10^4 cells/cm^2) in Dulbecco's Modified Eagles Medium (DMEM) supplemented with L-glutamine (2 mM), sodium pyruvate (1 mM), non-essential amino acids (1% v/v, Sigma) and heat-inactivated fetal calf serum (10% v/v) and incubated at 37°C in air containing 5% CO_2. One day after seeding, the medium was removed and the cells were then incubated in serum free-DMEM containing bovine serum albumin (0.25% w/v) and supplements (L-glutamine, sodium pyruvate and non-essential amino acids) for a further 24 h before the addition of human FX or FXa (Haemotologic Technologies) or plasma, collected from healthy donors. Pharmacological inhibitors were added to cell culture medium at a final concentration of 10 μM, 30 min prior to FXa and/or plasma incubation. All cells including controls were exposed to 0.1 % v/v of DMSO, the diluent for these inhibitors. The inhibitors used were: Apixaban (Euroasia Chemicals) for FXa, SCH79797 (300 nM, Tocris) for PAR-1 and PD98059 (Cell Signaling Technology) for ERK1/2. In selected experiments, FXa/plasma-treated cells were co-incubated with the following IgGs (Santa Cruz Biotechnology, 2 μg/mL): anti-annexin A2 (H-50), anti-PAR-1 (ATAP2) or control IgG.

In vivo murine model

The murine model of bleomycin-induced lung injury and inflammation was conducted as described previously (25). C57Bl/6 annexin A2 -/- mice were a generous gift of Prof Katherine Hajjar and Dr Min Luo (Cornell University, USA) (29) and bred in our animal facility. C57Bl/6 wild-type (WT) mice were obtained from the Animal Resources Centre, Perth, Australia. The experiments were performed with the approval from the Animal Experimentation Ethics Committee (AEC#1011588) of the University of Melbourne, following guidelines from the National Health and Medical Research Council. Mice (10-16 weeks) were divided into groups (n=4-11), comprising 40-60% females for groups administered a single intranasal instillation of bleomycin (4 U/Kg) (t=0 day). On the indicated days after bleomycin administration, mice were euthanized with pentobarbital (600 mg/kg, *i.p.*). BALF was then collected as described previously (52) before lungs were removed and frozen in liquid nitrogen or fixed in formalin for later analysis. To determine cell numbers in BALF, cells were stained with ethidium bromide and acridine orange before counting with the aid of a haemocytometer.

Immunohistochemistry (IHC)

Paraffin-embedded sections of human parenchymal lung tissue were immunohistochemically stained for antigens or histologically stained for collagen using Masson's Trichrome. Antigen was identified by rabbit polyclonal antibodies to annexin A2 or α-smooth muscle actin (Santa Cruz Biotechnology Inc, Dallas, TX, USA). Antibody staining was completed using the Dako EnVision anti-rabbit kit as appropriate (Dako Corp., Carpinteria, CA, USA) and 3,3'-diaminobenzidine (Sigma-Aldrich, St Louis, MO, USA); where sections were counterstained with hematoxylin.

Cell enumeration

After 48 h incubation with FX(a) or plasma, attached cells in 24 well plates were dissociated and harvested by incubation with trypsin (0.125% w/v) and EDTA (0.02% w/v) in PBS. Cells were

150 resuspended in 0.25% v/v BSA in PBS containing trypan blue (0.2% w/v) and viable cells counted
151 (in duplicate) with the aid of a hemocytometer.
152 *siRNA transfection*
153 Cells were seeded in 24 well plates (2.5 x 10^4 cells/cm^2) in antibiotic-free serum containing DMEM
154 and transfected 20 h later with 30 nM RNA short interference (siRNA) duplex oligonucleotides
155 using RNA*i*Max Lipofectamine (Invitrogen, CA, USA). Cells were incubated with Lipofectamine-
156 siRNA complex for 6 h, before incubation in serum-free DMEM 20 h prior to FXa addition.
157 Annexin A2 and control siRNA (Invitrogen, CA, USA) were used in the study. The following
158 siRNA sequence for annexin A2 was used: 5'-GCGACUACCAGAAAGCGCUGCUGUA-3'.
159
160 *Measurement of IL-6*
161 Levels of IL-6 in LF supernatants or BALF were measured by specific sandwich enzyme-linked
162 immunosorbent assays (ELISA) using commercial kits for human or mouse IL-6 (BD Biosciences,
163 CA, USA). Aliquots of culture supernatants were collected 24 h after addition of FXa/plasma for
164 assay of IL-6.
165
166 *Cell surface elution of annexin A2*
167 Annexin A2 is a calcium-dependent phospholipid binding protein which binds to the negatively-
168 charged cell surface via calcium chelation (13). EGTA-membrane extracts were prepared from LFs
169 grown in 6 well plates. Cells were washed two times with PBS before being maintained in PBS
170 (0.2 mL) containing 20 mM EGTA for 10 min. The supernatants were then collected, centrifuged at
171 1100*g* for 5 min before the annexin A2 of the supernatants were detected by immunoblotting.
172
173 *Real-time polymerase chain reaction (PCR)*
174 Real time PCR was conducted as previously described (42). RNA was purified from cells
175 maintained in 24 well culture plates using Trizol (Invitrogen), according to the manufacturer's
176 instructions. RNA was extracted from lung tissue using RNeasy mini prep columns (Qiagen),

177 according to the manufacturer's instructions. Before RNA extraction, frozen tissue was crushed
178 using a mortar and pestle in liquid N_2 to prevent thawing. Reverse transcription of total RNA and
179 the subsequent real-time polymerase chain reaction using an ABI Prism 7900HT sequence detection
180 system (Applied Biosystems) with the relevant forward and reverse primers were conducted as
181 previously described (42). The following primers were used: human annexin A2, 5'-
182 ACCTGGTTCAGTGCA TTCAGAA-3' (sense) and 5'-ACAGCCGATCAGCAAAATACAG-3'
183 (antisense); mouse Col1α1, 5'-ACGGCTGCACGAGTCACAC-3' (sense) and 5'- GGCAGG
184 CGGGAGGTCTT-3' (antisense) (20); mouse CTGF, 5'-GTCAAGCTGCCTGGGAAATG-3'
185 (sense) and 5'- CTTGGGCTCGTCACACACC-3' (antisense); human 18S ribosomal RNA (18S
186 rRNA) 5'-CGCCGCTAGAGGTGAAATTC-3' (sense) and 5'-RPTTGGCAAATGCTTTCGCTC-
187 3' (antisense); and mouse 18S rRNA, 5'-TCCGGCGAGGGAGCCTG-3' (sense) and 5'-
188 CCTGCTGCCTTCCTTGGAT-3' (antisense). The threshold cycle (CT) value determined for each
189 gene of each sample was normalized against that obtained for 18S rRNA, which was included as
190 internal control. For each sample, the level of mRNA for a particular gene is proportional to $2^{-(\Delta CT)}$,
191 where ΔCT is equal to the CT value of the target gene minus the CT value of 18S rRNA.
192
193 *Western blotting (cell lysates, conditioned media and EGTA eluents)*
194 Antigen in cell lysates (annexin A2, phospho-p44/42 ERK 1/2 and total ERK 1/2), the conditioned
195 media (annexin A2 and FXa) and EGTA eluents (annexin A2) of LFs were detected by
196 immunoblotting. Samples were subjected to SDS polyacrylamide gel electrophoresis (SDS-PAGE)
197 and electroblotted as described previously (40). Following electroblotting, membranes were
198 blocked with 5% skim milk in TBS-T (10 mM Tris; 75 mM NaCl; 0.1% Tween-20; pH 7.4) for 1 h.
199 Membranes were incubated overnight at 4°C with anti-phospho-p44/42 ERK 1/2 (#9101, rabbit
200 polyclonal IgG, 1:1000, Cell Signaling Technologies) (12), anti-annexin A2 (Z014, mouse
201 monoclonal IgG, 1:1000, Life Technologies), or anti-FXa (ab180701, rabbit polyclonal IgG,
202 1:1000, Abcam) diluted in 3% bovine serum albumin in TBS-T. Blots were washed three times

with TBS-T prior to incubation with secondary antibody, goat anti-mouse (Chemicon) or sheep anti-rabbit (Chemicon) IgG-horse raddish peroxidase conjugate, diluted 1:5000 in 5% skim milk/TBS-T for 1 h at room temperature. After three washes with TBS-T, antigen was detected by enhanced chemiluminescence (Amersham Biosciences, UK) using a BioRad Gel Doc imaging system. For the phospho-ERK immunoblots, the membranes were then stripped by incubation with 30 mL of 0.1 M glycine solution (pH 2.9) for 1 h at room temperature, blocked and incubated with primary anti-ERK 1/2 (SC-93, goat polyclonal IgG, 1:1000, Santa Cruz Biotechnology Inc) (9). Annexin A2 immunoblots of cell lysates were stripped and reprobed with anti-β-tubulin (AA2, mouse monoclonal IgG, 1:10,000, Millipore). Subsequent washes, secondary antibody incubation and chemiluminescence were as described above.

Western blotting (lung lysates)

Annexin A2 and GAPDH were immunodetected in lysates of lung tissue by infrared detection. Lysates (4.5 μg per lane) were subjected to electrophoresis and electroblotting as described for conditioned media and EGTA eluents. Each blot was probed at the same time with mouse, anti-annexin A2 (Z014, 1:1000, Life Technologies) and rabbit, anti-human GAPDH (ab9485; 1:2500; Abcam). Following co-incubation with anti-mouse 790 nm and anti-rabbit 680 nm IgG (1:10000, Abcam), immunoblots were imaged by infrared detection using an Odyssey scanner (Li-Cor, USA).

FXa enzyme activity

FXa enzyme activity was measured using a chromogenic substrate, Pefachrome FXa (Sigma). FXa (0.6-22 nM) in the presence of apixaban (10 μM) was incubated with 0.4 mM Pefachrome in Tris-HCl buffer (50 mM Tris; 2.5 mM $CaCl_2$; pH 8.4) at 37°C. Absorbance at 405 nm was monitored to assess FXa enzyme activity.

Statistical analysis

Data are presented as the mean ± SEM for *n* individual experiments, each experiment being conducted using cells, tissue or plasma from separate donors. All quantitative data, using Graphpad Prism 5.0 (Graphpad, San Diego, CA), were statistically analyzed by two-way analysis of variance (ANOVA) with repeated measures (except where stated otherwise) and treatment groups compared with Bonferroni's *post-hoc* tests. A value of $P<0.05$ was considered to be statistically significant.

Results

Annexin A2 is associated with fibroblasts in lung of IPF patients

The presence and distribution of annexin A2 in fibrotic lung from IPF patients was examined. Annexin A2 immunoreactivity was readily detected by IHC in the consolidated regions of lung tissue from IPF patients (**Fig. 1 a-d, g-i**). Annexin A2 was associated with flattened elongate fibroblasts in lung tissue of IPF patients, and with epithelial cells of intact alveoli in control tissue (**Fig. 1 e-f & j**). In serial sections of lung tissue from IPF patients, the distribution of annexin A2 immunoreactivity in IPF lung overlapped with that of the differentiated myofibroblast/myoepithelial marker, α-smooth muscle actin (α-SMA) (**Fig. 2 a-d**). Absolute levels of annexin A2 in lung lysates as detected by immunoblotting were lower in IPF (n=5) than controls (n=5) ($P<0.05$) (**Fig. 2 e-f**).

FXa regulates LF function in an annexin A2-dependent manner

The role of annexin A2 in mediating the fibrogenic actions of FXa on human lung fibroblasts (LFs) *in vitro* was investigated. Incubation of LFs from control donors with FXa (15-50 nM) increased IL-6 production and cell number ($P<0.05$, n=5), whereas FX zymogen (1.5-50 nM) had no effect ($P>0.05$, n=5) (**Fig. 3a-b**). Transfection of LFs with annexin A2 siRNA attenuated increases in IL-6 levels and cell number following incubation with FXa (15 nM) ($P<0.05$, n=5-6) (**Fig. 3c-d**). Levels of annexin A2 mRNA were reduced by annexin A2 siRNA by >80% ($P<0.05$, n=6) (**Fig. 3e**). A reduction in extracellular annexin A2, detected in both the conditioned media and EGTA-membrane extracts of siRNA-transfected LFs, was shown by immunoblotting (**Fig. 3f**). Targeting extracellular annexin A2 using neutralizing IgG (2 μg mL^{-1}) had similar effects to siRNA ($P<0.05$, n=6-11) (**Fig. 3g-h**).

IPF-derived LFs produce more IL-6 in response to FXa

The fibrogenic actions of FXa on LFs from IPF patients and controls were next compared. FXa-stimulated IL-6 production by IPF-derived LFs was greater than controls ($P<0.05$) (**Fig. 4a**), whereas the mitogenic effects of FXa were not different ($P>0.05$) (**Fig. 4b**). Whilst annexin A2 gene expression in LFs of IPF patients and controls were similar ($P>0.05$) (**Fig. 4c**), higher levels of annexin A2 were detected in the conditioned media of the IPF-derived cells (**Fig. 4d**).

FXa-stimulated IL-6 production and proliferation involves PAR-1

The cell-mediated actions of FXa involve PAR-1 activation. Pre-treatment of LFs with the selective PAR-1 antagonist, SCH79797 (0.3 μM) (41) attenuated FXa-stimulated increases in IL-6 production and cell number ($P<0.05$, n=5-6) (**Fig. 5a-b)**. These fibrogenic actions of FXa were also attenuated by targeting PAR-1 using neutralizing IgG (2 μg mL^{-1}) ($P<0.05$, n=5) (**Fig. 5c-d**).

FXa-evoked actions are regulated by MAPK signal-transduction

Activation of PAR-1 by FXa stimulates the ERK1/2 (MAPK) signal transduction pathway in endothelial and smooth muscle cells (4, 41). In this study, FXa (15 nM) stimulated increased ERK1/2 phosphorylation in LFs within 5 min of addition ($P<0.05$, n=5) (**Fig. 6a-b**). Incubation with either anti-annexin A2 or -PAR-1 IgG, or pre-treatment with SCH79797 attenuated FXa-stimulated ERK1/2 phosphorylation (**Fig. 6c-e**). Inhibition of ERK1/2 phosphorylation with PD98059 (10 μM) (41) attenuated FXa-induced IL-6 release and fibroblast proliferation ($P<0.05$, n=5) (**Fig. 6f-g**).

The fibrogenic actions of plasma involve FXa and annexin A2

LFs would be exposed to plasma-derived FX, with concentrations spiking during injury or disease exacerbation. Thus the fibrogenic actions of human plasma on LFs and the roles of FX and annexin A2 were examined. We show that FXa-stimulated IL-6 production and cell number was inhibited by the selective FXa inhibitor apixaban (10 μM) ($P<0.05$, n=3) (**Fig. 7a-b**). Incubation with human

286 plasma (5% v/v) had similar apixaban-sensitive effects ($P<0.05$, n=7) (**Fig. 7a-b**). Apixaban at 10
287 μM was shown to inhibit the enzymatic activity of purified FXa (**Fig. 7c**). Both FX and FXa were
288 detected in the conditioned media of LFs following incubation with plasma (**Fig. 7d**). The actions
289 of plasma were attenuated by incubation with either annexin A2 or PAR-1 neutralizing IgG (2 μg
290 mL^{-1}) ($P<0.05$, n=4) (**Fig. 7e-f**).
291
292 *Annexin A2 gene deletion reduces lung IL-6 production and fibrogenesis*
293 The role of annexin A2 in lung injury and fibrogenesis was examined *in vivo*. Bleomycin-induced
294 levels of IL-6 in the BALF were reduced in annexin A2 -/- mice compared to WT mice 3 days after
295 instillation (**Fig. 8a**). The effect of annexin A2 gene deletion on bleomycin-induced increases in
296 BALF total cell or macrophage number were observed on day 7 and thereafter, but not earlier on
297 day 3 (**Fig. 8b-d**). Bleomycin-induced increases in the expression of the fibrogenic genes, CTGF
298 and Col1α1 (t=14 d), were also reduced in annexin A2 -/- mice (**Fig. 8e-f**) ($P<0.05$, n=7-10).
299 Whilst there was no significant difference in lung hydroxproline (collagen) between WT and
300 annexin A2 -/- mice following bleomycin challenge, there was in lung dry weight (t=21 d) (**Fig. 8g-**
301 **h**).
302
303

Discussion

In this study, we provide evidence that annexin A2 contributes to lung injury and disease. Fibroblast annexin A2 was detected in lung tissue of IPF patients and the targeting of annexin A2 blunted a number of fibrogenic responses, but not lung collagen accumulation *in vivo*. Extracellular annexin A2 augmented fibrogenic IL-6 production and proliferation by human lung fibroblasts *in vitro*. Furthermore, FXa-stimulated increases in IL-6 were greater for lung fibroblasts of IPF donors than controls, and this corresponded to increased levels of extracellular annexin A2. Our data indicates that annexin A2 acts as a FXa-transducer, mediating the lung fibrogenic activity of FXa. Based on our novel findings we propose that extracellular annexin A2 of fibroblast origin potentially contributes to cytokine production and fibroproliferation in IPF.

Annexin A2 has pleiotropic functions depending on its location. Intracellular annexin A2 has roles in endocytosis, exocytosis, membrane trafficking, and redox-signalling (16), whereas extracellular annexin A2 regulates protease activation (*e.g.,* plasmin formation) and signalling (39, 49). Annexin A2 is implicated in a number of pathologies including cancer (19, 21, 57), anti-phospholipid syndrome (7), rheumatoid arthritis (55) and pulmonary infections (22, 48). Increased levels of annexin A2 in renal (14) and liver (56) fibrosis suggest a role in fibrotic disease. Interestingly, we showed protein levels of annexin A2 in lung tissue of IPF patients are lower than controls, an observation reported in a previous study (24). However, when defining the role of annexin A2 in IPF, other measures of annexin A2 activity such as cellular distribution, extracellular trafficking and post-translational modifications (*e.g*., N-terminal cleavage) need to be assessed. The decrease in absolute levels of annexin A2 in IPF may be a consequence of reduced intracellular annexin A2 in type II alveolar epithelial cells (AECIIs), where it plays an important role in surfactant release (47). Korfei *et al* reported intense cytoplasmic staining of annexin A2 in AECIIs of normal human lung, which was reduced in AECIIs in fibrotic lung in IPF (24). In the same study, bronchiolar basal cells in IPF lung showed increased annexin A2 cell surface expression, but the detection of annexin A2 in fibroblasts was not reported nor commented on (24). In the current study, IHC was used to

identify annexin A2 of fibroblasts in consolidated regions of lung tissue from IPF patients. The presence of detectable annexin A2 in α-SMA-immunoreactive fibroblasts is additional evidence that annexin A2 fibroblast production occurs in IPF.

The pathological contributions of annexin A2 are to a large part attributable to its extracellular functions. For example, the hypersecretion of annexin A2 in acute promyelocytic leukemia causes excessive fibrinolysis and haemorrhage (21), whereas in pancreatic ductal adenocarcinoma, extracellular annexin A2 is implicated in epithelial mesenchymal transition (57). Oxidative, radiation and heat stress all stimulate annexin A2 extracellular release (11, 51, 53). A potential mechanism by which extracellular annexin A2 contributes to fibrosis involves PAR-1, a G protein-coupled receptor implicated in pulmonary fibrosis (18, 35, 43). In the current study, FXa-stimulated IL-6 production and proliferation of lung fibroblasts was attenuated by PAR-1 neutralizing IgG or by pharmacological inhibition of PAR-1 or MAPK kinases downstream of PAR-1 (35). This is the first time to our knowledge that FXa, whether purified or present in plasma, has been shown to stimulate either of these fibrogenic responses in primary cultures of human lung fibroblasts. Targeting annexin A2 also attenuated the fibrogenic actions of FXa and plasma. Our data suggests that the FXa-binding annexin A2 acts as a FXa-transducer in activating PAR-1 on lung fibroblasts, as shown previously with endothelial cells (4) and smooth muscle (41). This effect may be through concentrating FXa at the cell surface by calcium binding or via its interactions with integrins (27). FXa-stimulated IL-6 production was greater for IPF-derived lung fibroblasts than controls, possibly a consequence of increased extracellular translocation of annexin A2. However, the effects of FXa on IPF and control lung fibroblast proliferation were similar in magnitude. The mitogenic actions of FXa may be blunted in IPF-derived lung fibroblasts because of accelerated replicative cellular senescence (54).

356 The effects of annexin A2 gene deletion on bleomycin-induced lung injury and fibrosis were also
357 investigated. Annexin A2 gene deletion reduced BALF levels of IL-6 on day 3, prior to any
358 detectable changes in BALF cellularity or fibrogenic gene expression. The decreased cellularity
359 observed on day 7 was attributable to a reduction in the number of macrophages rather than
360 neutrophils or lymphocytes (data not shown). Alveolar macrophages have an important role in lung
361 injury initiating and maintaining inflammation, as well as being involved in resolution and repair
362 (2). In another murine lung injury model featuring acute neutrophilic inflammation, annexin A2
363 gene deletion also had no effect on BALF cell number 24 h after intranasal instillation of endotoxin
364 (unpublished observations). It appears annexin A2 contributes less to the acute (*i.e.,* neutrophilic)
365 inflammatory response following lung injury, and more to the subsequent inflammatory and
366 fibrogenic phases. Whilst annexin A2 gene deletion reduced fibrogenic gene expression and dry
367 weight in lung of bleomycin-treated mice, the effect on collagen content was less than anticipated.
368 This may be explained by the effect of annexin A2 gene deletion on net collagen production as
369 being multifaceted, not just involving extracellular annexin A2. Intracellular annexin A2 is a
370 potential negative post-transcriptional regulator of type I collagen synthesis (36). Whilst the
371 contribution of FXa to the fibrogenic actions of annexin A2 *in vivo* were not ascertained in this
372 study, it has been shown that experimental lung fibrosis is blunted by the selective inhibition of FXa
373 (43).

374

375 Data from our study suggests that the fibrogenic role of annexin A2 involves IL-6. Not only did
376 annexin A2 induce lung fibroblast IL-6 production *in vitro*, but annexin A2 gene deletion also
377 attenuated bleomycin-induced increases in the levels of IL-6 detected in BALF *in vivo*. IL-6 is a
378 fibrogenic cytokine which signals through glycoprotein 130 (gp130) and is implicated in pulmonary
379 fibrosis (23). IL-6 levels in serum and BALF of patients with ARDS and ILDs are elevated, being
380 predictive of lung function decline and mortality (10, 15, 28, 50). IL-6 immunoreactivity is also
381 associated with fibroblasts in lung tissue of IPF patients (1, 38). Lung fibroblasts exposed to lung

edema fluid from patients with early stage ARDS produce increased IL-6, which in turn stimulates fibroblast activation and proliferation in an autocrine manner via gp130 signaling (32). We found that plasma from healthy individuals exhibited similar effects on lung fibroblasts as purified FXa and were attenuated by apixaban. Active FXa was detected in the culture supernatants of lung fibroblasts following incubation with plasma, suggesting that these cells convert plasma-borne FX into FXa.

Selectively targeting annexin A2 to inhibit its fibrogenic actions is a potential therapeutic strategy to treat IPF. Withaferin A, a plant-derived compound which binds to the N terminus of annexin A2 (34) is protective in experimental models of injury, including isoproterenol-induced myocardial fibrosis (8). Another potential therapeutic, TM601, a synthetic polypeptide, reduces ocular neovascularization and vascular leakage *in vivo,* via binding annexin A2 (26). As an emerging therapeutic target for cancer, it is likely that more highly selective small molecule inhibitors of annexin A2 will be developed and/or investigated in pre-clinical and clinical studies (37). The extracellular compartmentalization of annexin A2 in fibrosis allows for targeting by antibody based-therapy. Such therapy would be advantageous in that it does not interfere with the intracellular roles of annexin A2 (47). Annexin A2 neutralization using antibody therapy has been validated in murine cancer models *in vivo*, inhibiting tumour growth/metastasis without evidence of toxicity (45, 46, 57).

Our study provides novel insights into the role of annexin A2 in lung pathology. The detrimental contribution of annexin A2 is attributable to an extracellular location, where it acts as a transducer for FXa. Furthermore, our finding that annexin A2 gene deletion reduces lung fibrogenic processes *in vivo* provides proof-of-concept evidence that annexin A2 is a potential therapeutic target for disorders such as IPF.

Author contributions

Concept and design: MS, AGS, PVSL, GW; acquisition, analysis and interpretation of data: MS, SL, AB, DW, TH, JJ, AGS, CG; and drafting the manuscript for important intellectual content: MS, AGS, DK, GW.

Acknowledgments

This work was supported by the NHMRC (Australia) research grant #1022048, #1059655, #1045372 and #1099569. Additional support was from the John Hunter Hospital Charitable Trust Fund. We thank the Departments of Respiratory Medicine, Surgery, and Anatomical Pathology, Alfred Hospital, Australia, and Prof. Catriona MacClean for assistance in obtaining human lung tissue.

419 **Figure Legends**

420 ***Figure 1.*** **Annexin A2 immunoreactivity in lung tissue of IPF patients.** (a, c, e) Serial sections
421 of parenchymal tissue from an IPF patient (ALF019) and control (ALF009) immunostained for
422 annexin A2. (b, d, f) Negative IgG controls of serial sections from the same lung tissue. (g-j) Lung
423 sections from three additional IPF patients (ALF028, ALF016 and ALF023) and control (ALF013)
424 immunostained for annexin A2. The IPF sections show annexin A2 staining (brown) in flattened
425 elongate fibroblasts (Fb). Annexin A2 immunoreactivity was also associated with epithelial cells
426 (Ep) in control tissue. The scale bars in the images are (a, b) 80, (c, d) 300, (e, f) 200 or (g-j) 100
427 micron.

428

429 ***Figure 2.*** **Annexin A2 distribution in fibrotic lung overlaps with α-SMA.** Sequential serial
430 lung tissue sections from an IPF patient (ALF027) and control (ALF024) comparing (a, c) annexin
431 A2 immunostaining with (b, d) α-SMA. The scale bar in the images are 100 (a, b) or 200 (c, d)
432 micron. (e, f) Immunoblots and densitometry analysis of annexin A2 and GAPDH in tissue lysates
433 of lung from IPF (ALF008, ALF016, ALF019, ALF023 and ALF027) and control (ALF012,
434 ALF013, ALF017, ALF024 and ALF25) donors. For lung tissue, 4.5 μg of protein was loaded per
435 lane. Densitometry data (annexin A2/GAPDH ratios) of lung tissue samples were analyzed by a
436 Mann Whitney test (*$P<0.05$).

437

438 ***Figure 3.*** **Factor Xa stimulates fibrogenic function in an annexin A2-dependent manner.** (a)
439 Level of IL-6 and (b) cell number in LF cultures (from control donors) incubated with FX or FXa
440 for 24 h (IL-6) or 48 h (cell number). Under basal conditions, the level of IL-6 and cell number
441 were 1.64 ± 0.36 ng mL^{-1} and 50,100 ± 7,258 per well respectively. (c, d) IL-6 levels and cell
442 number in LF cultures following annexin A2 siRNA transfection and incubation with FXa (15 nM)
443 (n=5-6). (e) Levels of annexin A2 mRNA in siRNA-transfected LFs (n=6). (f) Representative
444 immunoblot of annexin A2 in the EGTA membrane extracts and conditioned media of LFs (IPF)

following siRNA transfection. Equal volumes (20 μL) of EGTA eluent and media were subject to electrophoresis. The volumes of EGTA extracts and media obtained from LFs grown in wells of 6 well plates were 0.2 and 2 mL respectively. (g, h) IL-6 production and cell number in LFs incubated with FXa (15 nM) and anti-annexin A2 or isotype control antibody (2 μg mL^{-1}) (n=6). All data were analyzed by two-way repeated measures ANOVA and Bonferroni's post-test except mRNA data which was analyzed by student's t test (*P<0.05, **P<0.01).

Figure 4. **FXa-stimulated IL-6 production is greater in LFs of IPF patients.** (a) The effects of FXa (15 nM) on IL-6 production by LFs of IPF (n=6) and control (n=11) donors. (b) FXa effects on proliferation of LFs from IPF (n=5) and control (n=5) donors. (c) Relative levels of annexin A2 mRNA in LFs of IPF patients (n=7) and controls (n=7). (d) Annexin A2 levels in the conditioned media (top) and cell lysates (bottom) of IPF-derived LFs and controls grown in 24 well plates (0.5 mL media). 15 μL of media and 4 μg of cell lysate protein were subjected to SDS-PAGE. Data (a-c) were analyzed by Mann Whitney test (*P<0.05).

Figure 5. **FXa actions are mediated by PAR-1.** (a-b) IL-6 levels and cell number in LF cultures following incubation with FXa (15 nM) and SCH79797 (300 nM) or vehicle control (n=5-6). (c-d) The effect of anti-PAR-1 or isotype control antibody (2 μg mL^{-1}) on the fibrogenic actions of FXa (n=6). Data were analyzed by two-way repeated measures ANOVA and Bonferroni's post-test *(*P<0.05, **P<0.01).

Figure 6. **FXa actions are mediated by MAPK signaling.** (a-b) Time-course of ERK1/2-phosphorylation following incubation with FXa (15 nM). (c-e) Representative immunoblots showing effect of neutralizing IgGs or SCH79797 (300 nM) on ERK1/2 phosphorylation after 30 min FXa incubation. (f-g) The effect of the kinase inhibitor, PD98059 (10 μM) on levels of IL-6 and cell number after FXa incubation. Densitometry data (ERK-P/ERK_{total} ratios) were analyzed by

one-way repeated measures ANOVA and Dunn's post-test (*P<0.05 versus control, n=7). Data (f-g) was analyzed by two-way repeated measures ANOVA and Bonferroni's post-test (*P<0.05, **P<0.01, n=5).

Figure 7. **The fibrogenic actions of plasma involve FXa and annexin A2.** (a, b) IL-6 levels and cell number in lung fibroblast cultures incubated with either FXa (15 nM) or human plasma (5% v/v) in the absence or presence of apixaban (10 μM) (P<0.05, n=5). (c) The effect of apixaban (10 μM) on the enzyme activity of purified FXa. (d) Immunoblot showing FX(a) immunoreactivity in the conditioned media of LFs or culture media in the absence of cells, incubated with plasma (pl, 5% v/v) for 4 h. The FX antibody used in the study recognises the heavy weight chain of FX. The heavy chain components of FXa and FX zymogen have ~molecular weights of 30 and 42 kDa respectively. (e, f) The actions of plasma on LFs in the presence of annexin A2 or PAR-1 neutralizing IgG (2 $\mu g.mL^{-1}$) (P<0.05, n=5).

Figure 8. **Annexin A2 gene deletion attenuates bleomycin-induced increases in lung inflammation and fibrogenic gene expression.** Levels of (a) IL-6 (t=3d) and numbers of (b-c) total cells (t=3 and 7d) and (d) macrophages (t=7d) in the BALF of wild-type (WT) and annexin A2 -/- mice after treatment with bleomycin (4 U/Kg) or saline vehicle. Levels of (e) CTGF and (f) Col1α1 (t=14d) and the (g) hydroxyproline content and (h) dry weight (t=21d) of lung tissue. Data were analyzed by two-way repeated measures ANOVA and Bonferroni's post-test *P<0.05, **P<0.01 (n=4-12).

References

1. **Abdul-Hafez A, Shu R, and Uhal BD**. JunD and HIF-1alpha mediate transcriptional activation of angiotensinogen by TGF-beta1 in human lung fibroblasts. *FASEB journal : official publication of the Federation of American Societies for Experimental Biology* 23: 1655-1662, 2009.
2. **Aggarwal NR, King LS, and D'Alessio FR**. Diverse macrophage populations mediate acute lung inflammation and resolution. *American journal of physiology Lung cellular and molecular physiology* 306: L709-725, 2014.
3. **Ahluwalia N, Shea BS, and Tager AM**. New therapeutic targets in idiopathic pulmonary fibrosis. Aiming to rein in runaway wound-healing responses. *American journal of respiratory and critical care medicine* 190: 867-878, 2014.
4. **Bhattacharjee G, Ahamed J, Pawlinski R, Liu C, Mackman N, Ruf W, and Edgington TS**. Factor Xa binding to annexin 2 mediates signal transduction via protease-activated receptor 1. *Circulation research* 102: 457-464, 2008.
5. **Blanc-Brude OP, Archer F, Leoni P, Derian C, Bolsover S, Laurent GJ, and Chambers RC**. Factor Xa stimulates fibroblast procollagen production, proliferation, and calcium signaling via PAR1 activation. *Exp Cell Res* 304: 16-27, 2005.
6. **Burnham EL, Janssen WJ, Riches DW, Moss M, and Downey GP**. The fibroproliferative response in acute respiratory distress syndrome: mechanisms and clinical significance. *The European respiratory journal* 43: 276-285, 2014.
7. **Cesarman-Maus G, Cantu-Brito C, Barinagarrementeria F, Villa R, Reyes E, Sanchez-Guerrero J, Hajjar KA, and Latorre EG**. Autoantibodies against the fibrinolytic receptor, annexin A2, in cerebral venous thrombosis. *Stroke; a journal of cerebral circulation* 42: 501-503, 2011.
8. **Challa AA, Vukmirovic M, Blackmon J, and Stefanovic B**. Withaferin-A reduces type I collagen expression in vitro and inhibits development of myocardial fibrosis in vivo. *PLoS One* 7: e42989, 2012.
9. **Chen G, Ghosh P, and Longo DL**. Distinctive mechanism for sustained TGF-beta signaling and growth inhibition: MEK1 activation-dependent stabilization of type II TGF-beta receptors. *Molecular cancer research : MCR* 9: 78-89, 2011.
10. **De Lauretis A, Sestini P, Pantelidis P, Hoyles R, Hansell DM, Goh NS, Zappala CJ, Visca D, Maher TM, Denton CP, Ong VH, Abraham DJ, Kelleher P, Hector L, Wells AU, and Renzoni EA**. Serum interleukin 6 is predictive of early functional decline and mortality in interstitial lung disease associated with systemic sclerosis. *The Journal of rheumatology* 40: 435-446, 2013.
11. **Deora AB, Kreitzer G, Jacovina AT, and Hajjar KA**. An annexin 2 phosphorylation switch mediates p11-dependent translocation of annexin 2 to the cell surface. *J Biol Chem* 279: 43411-43418, 2004.
12. **Escuin-Ordinas H, Li S, Xie MW, Sun L, Hugo W, Huang RR, Jiao J, de-Faria FM, Realegeno S, Krystofinski P, Azhdam A, Komenan SM, Atefi M, Comin-Anduix B, Pellegrini M, Cochran AJ, Modlin RL, Herschman HR, Lo RS, McBride WH, Segura T, and Ribas A**. Cutaneous wound healing through paradoxical MAPK activation by BRAF inhibitors. *Nature communications* 7: 12348, 2016.
13. **Fang YT, Lin CF, Wang CY, Anderson R, and Lin YS**. Interferon-gamma stimulates p11-dependent surface expression of annexin A2 in lung epithelial cells to enhance phagocytosis. *Journal of cellular physiology* 227: 2775-2787, 2012.
14. **Feighery R, Maguire P, Ryan MP, and McMorrow T**. A proteomic approach to immune-mediated epithelial-mesenchymal transition. *Proteomics Clinical applications* 2: 1110-1117, 2008.
15. **Frenzel J, Gessner C, Sandvoss T, Hammerschmidt S, Schellenberger W, Sack U, Eschrich K, and Wirtz H**. Outcome prediction in pneumonia induced ALI/ARDS by clinical features and peptide patterns of BALF determined by mass spectrometry. *PloS one* 6: e25544, 2011.
16. **Hajjar KA**. The Biology of Annexin A2: From Vascular Fibrinolysis to Innate Immunity. *Transactions of the American Clinical and Climatological Association* 126: 144-155, 2015.

17. **Hedhli N, Falcone DJ, Huang B, Cesarman-Maus G, Kraemer R, Zhai H, Tsirka SE, Santambrogio L, and Hajjar KA**. The Annexin A2/S100A10 System in Health and Disease: Emerging Paradigms. *J Biomed Biotechnol* 2012: 406273, 2012.
18. **Howell DC, Johns RH, Lasky JA, Shan B, Scotton CJ, Laurent GJ, and Chambers RC**. Absence of proteinase-activated receptor-1 signaling affords protection from bleomycin-induced lung inflammation and fibrosis. *Am J Pathol* 166: 1353-1365, 2005.
19. **Inokuchi J, Narula N, Yee DS, Skarecky DW, Lau A, Ornstein DK, and Tyson DR**. Annexin A2 positively contributes to the malignant phenotype and secretion of IL-6 in DU145 prostate cancer cells. *Int J Cancer* 124: 68-74, 2009.
20. **Kenyon NJ, Ward RW, McGrew G, and Last JA**. TGF-beta1 causes airway fibrosis and increased collagen I and III mRNA in mice. *Thorax* 58: 772-777, 2003.
21. **Kim J, and Hajjar KA**. Annexin II: a plasminogen-plasminogen activator co-receptor. *Front Biosci* 7: d341-348, 2002.
22. **Kirschnek S, Adams C, and Gulbins E**. Annexin II is a novel receptor for Pseudomonas aeruginosa. *Biochemical and biophysical research communications* 327: 900-906, 2005.
23. **Knight DA, Ernst M, Anderson GP, Moodley YP, and Mutsaers SE**. The role of gp130/IL-6 cytokines in the development of pulmonary fibrosis: critical determinants of disease susceptibility and progression? *Pharmacol Ther* 99: 327-338, 2003.
24. **Korfei M, Schmitt S, Ruppert C, Henneke I, Markart P, Loeh B, Mahavadi P, Wygrecka M, Klepetko W, Fink L, Bonniaud P, Preissner KT, Lochnit G, Schaefer L, Seeger W, and Guenther A**. Comparative proteomic analysis of lung tissue from patients with idiopathic pulmonary fibrosis (IPF) and lung transplant donor lungs. *Journal of proteome research* 10: 2185-2205, 2011.
25. **Langenbach SY, Wheaton BJ, Fernandes DJ, Jones C, Sutherland TE, Wraith BC, Harris T, Schuliga MJ, McLean C, and Stewart AG**. Resistance of fibrogenic responses to glucocorticoid and 2-methoxyestradiol in bleomycin-induced lung fibrosis in mice. *Canadian journal of physiology and pharmacology* 85: 727-738, 2007.
26. **Lima e Silva R, Shen J, Gong YY, Seidel CP, Hackett SF, Kesavan K, Jacoby DB, and Campochiaro PA**. Agents that bind annexin A2 suppress ocular neovascularization. *Journal of cellular physiology* 225: 855-864, 2010.
27. **Lin L, Wu C, and Hu K**. Tissue plasminogen activator activates NF-kappaB through a pathway involving annexin A2/CD11b and integrin-linked kinase. *J Am Soc Nephrol* 23: 1329-1338, 2012.
28. **Lin WC, Lin CF, Chen CL, Chen CW, and Lin YS**. Prediction of outcome in patients with acute respiratory distress syndrome by bronchoalveolar lavage inflammatory mediators. *Exp Biol Med (Maywood)* 235: 57-65, 2010.
29. **Ling Q, Jacovina AT, Deora A, Febbraio M, Simantov R, Silverstein RL, Hempstead B, Mark WH, and Hajjar KA**. Annexin II regulates fibrin homeostasis and neoangiogenesis in vivo. *The Journal of clinical investigation* 113: 38-48, 2004.
30. **MacLeod TJ, Kwon M, Filipenko NR, and Waisman DM**. Phospholipid-associated annexin A2-S100A10 heterotetramer and its subunits: characterization of the interaction with tissue plasminogen activator, plasminogen, and plasmin. *The Journal of biological chemistry* 278: 25577-25584, 2003.
31. **Mercer PF, Johns RH, Scotton CJ, Krupiczojc MA, Konigshoff M, Howell DC, McAnulty RJ, Das A, Thorley AJ, Tetley TD, Eickelberg O, and Chambers RC**. Pulmonary epithelium is a prominent source of proteinase-activated receptor-1-inducible CCL2 in pulmonary fibrosis. *American journal of respiratory and critical care medicine* 179: 414-425, 2009.
32. **Olman MA, White KE, Ware LB, Simmons WL, Benveniste EN, Zhu S, Pugin J, and Matthay MA**. Pulmonary edema fluid from patients with early lung injury stimulates fibroblast proliferation through IL-1 beta-induced IL-6 expression. *J Immunol* 172: 2668-2677, 2004.
33. **Ortiz-Stern A, Deng X, Smoktunowicz N, Mercer PF, and Chambers RC**. PAR-1-dependent and PAR-independent pro-inflammatory signaling in human lung fibroblasts exposed to thrombin. *Journal of cellular physiology* 227: 3575-3584, 2012.

34. **Ozorowski G, Ryan CM, Whitelegge JP, and Luecke H**. Withaferin A binds covalently to the N-terminal domain of annexin A2. *Biological chemistry* 393: 1151-1163, 2012.
35. **Pendurthi UR, Ngyuen M, Andrade-Gordon P, Petersen LC, and Rao LV**. Plasmin induces Cyr61 gene expression in fibroblasts via protease-activated receptor-1 and p44/42 mitogen-activated protein kinase-dependent signaling pathway. *Arteriosclerosis, thrombosis, and vascular biology* 22: 1421-1426, 2002.
36. **Schafer G, Hitchcock JK, Shaw TM, Katz AA, and Parker MI**. A novel role of annexin A2 in human type I collagen gene expression. *Journal of cellular biochemistry* 116: 408-417, 2015.
37. **Schuliga M**. The Inflammatory Actions of Coagulant and Fibrinolytic Proteases in Disease. *Mediators of inflammation* 2015: 437695, 2015.
38. **Schuliga M, Jaffar J, Harris T, Knight DA, Westall G, and Stewart AG**. The fibrogenic actions of lung fibroblast-derived urokinase: a potential drug target in IPF. *Scientific reports* 7: 41770, 2017.
39. **Schuliga M, Langenbach S, Xia YC, Qin C, Mok JS, Harris T, Mackay GA, Medcalf RL, and Stewart AG**. Plasminogen-stimulated inflammatory cytokine production by airway smooth muscle cells is regulated by annexin A2. *American journal of respiratory cell and molecular biology* 49: 751-758, 2013.
40. **Schuliga M, Ong SC, Soon L, Zal F, Harris T, and Stewart AG**. Airway smooth muscle remodels pericellular collagen fibrils: implications for proliferation. *American journal of physiology Lung cellular and molecular physiology* 298: L584-592, 2010.
41. **Schuliga M, Royce SG, Langenbach S, Berhan A, Harris T, Keenan CR, and Stewart AG**. The Coagulant Factor Xa Induces Protease-Activated Receptor-1 and Annexin A2-Dependent Airway Smooth Muscle Cytokine Production and Cell Proliferation. *American journal of respiratory cell and molecular biology* 54: 200-209, 2016.
42. **Schuliga MJ, See I, Ong SC, Soon L, Camoretti-Mercado B, Harris T, and Stewart AG**. Fibrillar collagen clamps lung mesenchymal cells in a nonproliferative and noncontractile phenotype. *American journal of respiratory cell and molecular biology* 41: 731-741, 2009.
43. **Scotton CJ, Krupiczojc MA, Konigshoff M, Mercer PF, Lee YC, Kaminski N, Morser J, Post JM, Maher TM, Nicholson AG, Moffatt JD, Laurent GJ, Derian CK, Eickelberg O, and Chambers RC**. Increased local expression of coagulation factor X contributes to the fibrotic response in human and murine lung injury. *The Journal of clinical investigation* 119: 2550-2563, 2009.
44. **Selman M, Thannickal VJ, Pardo A, Zisman DA, Martinez FJ, and Lynch JP, 3rd**. Idiopathic pulmonary fibrosis: pathogenesis and therapeutic approaches. *Drugs* 64: 405-430, 2004.
45. **Sharma M, Blackman MR, and Sharma MC**. Antibody-directed neutralization of annexin II (ANX II) inhibits neoangiogenesis and human breast tumor growth in a xenograft model. *Exp Mol Pathol* 92: 175-184, 2012.
46. **Sharma M, Ownbey RT, and Sharma MC**. Breast cancer cell surface annexin II induces cell migration and neoangiogenesis via tPA dependent plasmin generation. *Exp Mol Pathol* 88: 278-286, 2010.
47. **Singh TK, Abonyo B, Narasaraju TA, and Liu L**. Reorganization of cytoskeleton during surfactant secretion in lung type II cells: a role of annexin II. *Cellular signalling* 16: 63-70, 2004.
48. **Somarajan SR, Al-Asadi F, Ramasamy K, Pandranki L, Baseman JB, and Kannan TR**. Annexin A2 mediates Mycoplasma pneumoniae community-acquired respiratory distress syndrome toxin binding to eukaryotic cells. *mBio* 5: 2014.
49. **Stewart AG, Xia YC, Harris T, Royce S, Hamilton JA, and Schuliga M**. Plasminogen-stimulated airway smooth muscle cell proliferation is mediated by urokinase and annexin A2, involving plasmin-activated cell signalling. *British journal of pharmacology* 170: 1421-1435, 2013.
50. **Takizawa H, Satoh M, Okazaki H, Matsuzaki G, Suzuki N, Ishii A, Suko M, Okudaira H, Morita Y, and Ito K**. Increased IL-6 and IL-8 in bronchoalveolar lavage fluids (BALF) from patients with sarcoidosis: correlation with the clinical parameters. *Clin Exp Immunol* 107: 175-181, 1997.

51. **Tanaka T, Akatsuka S, Ozeki M, Shirase T, Hiai H, and Toyokuni S**. Redox regulation of annexin 2 and its implications for oxidative stress-induced renal carcinogenesis and metastasis. *Oncogene* 23: 3980-3989, 2004.
52. **Ward JE, Fernandes DJ, Taylor CC, Bonacci JV, Quan L, and Stewart AG**. The PPARgamma ligand, rosiglitazone, reduces airways hyperresponsiveness in a murine model of allergen-induced inflammation. *Pulmonary pharmacology & therapeutics* 19: 39-46, 2006.
53. **Weber TJ, Opresko LK, Waisman DM, Newton GJ, Quesenberry RD, Bollinger N, Moore RJ, and Smith RD**. Regulation of the low-dose radiation paracrine-specific anchorage-independent growth response by annexin A2. *Radiation research* 172: 96-105, 2009.
54. **Yanai H, Shteinberg A, Porat Z, Budovsky A, Braiman A, Ziesche R, and Fraifeld VE**. Cellular senescence-like features of lung fibroblasts derived from idiopathic pulmonary fibrosis patients. *Aging* 7: 664-672, 2015.
55. **Yi J, Zhu Y, Jia Y, Jiang H, Zheng X, Liu D, Gao S, Sun M, Hu B, Jiao B, Wang L, and Wang K**. The Annexin a2 Promotes Development in Arthritis through Neovascularization by Amplification Hedgehog Pathway. *PloS one* 11: e0150363, 2016.
56. **Zhang L, Peng X, Zhang Z, Feng Y, Jia X, Shi Y, Yang H, Zhang Z, Zhang X, Liu L, Yin L, and Yuan Z**. Subcellular proteome analysis unraveled annexin A2 related to immune liver fibrosis. *Journal of cellular biochemistry* 110: 219-228, 2010.
57. **Zheng L, Foley K, Huang L, Leubner A, Mo G, Olino K, Edil BH, Mizuma M, Sharma R, Le DT, Anders RA, Illei PB, Van Eyk JE, Maitra A, Laheru D, and Jaffee EM**. Tyrosine 23 phosphorylation-dependent cell-surface localization of annexin A2 is required for invasion and metastases of pancreatic cancer. *PLoS One* 6: e19390, 2011.
58. **Zhu W, Bi M, Liu Y, Wang Y, Pan F, Qiu L, Guo A, Lv H, Yao P, Zhang N, and Wang P**. Thrombin promotes airway remodeling via protease-activated receptor-1 and transforming growth factor-beta1 in ovalbumin-allergic rats. *Inhal Toxicol* 25: 577-586, 2013.

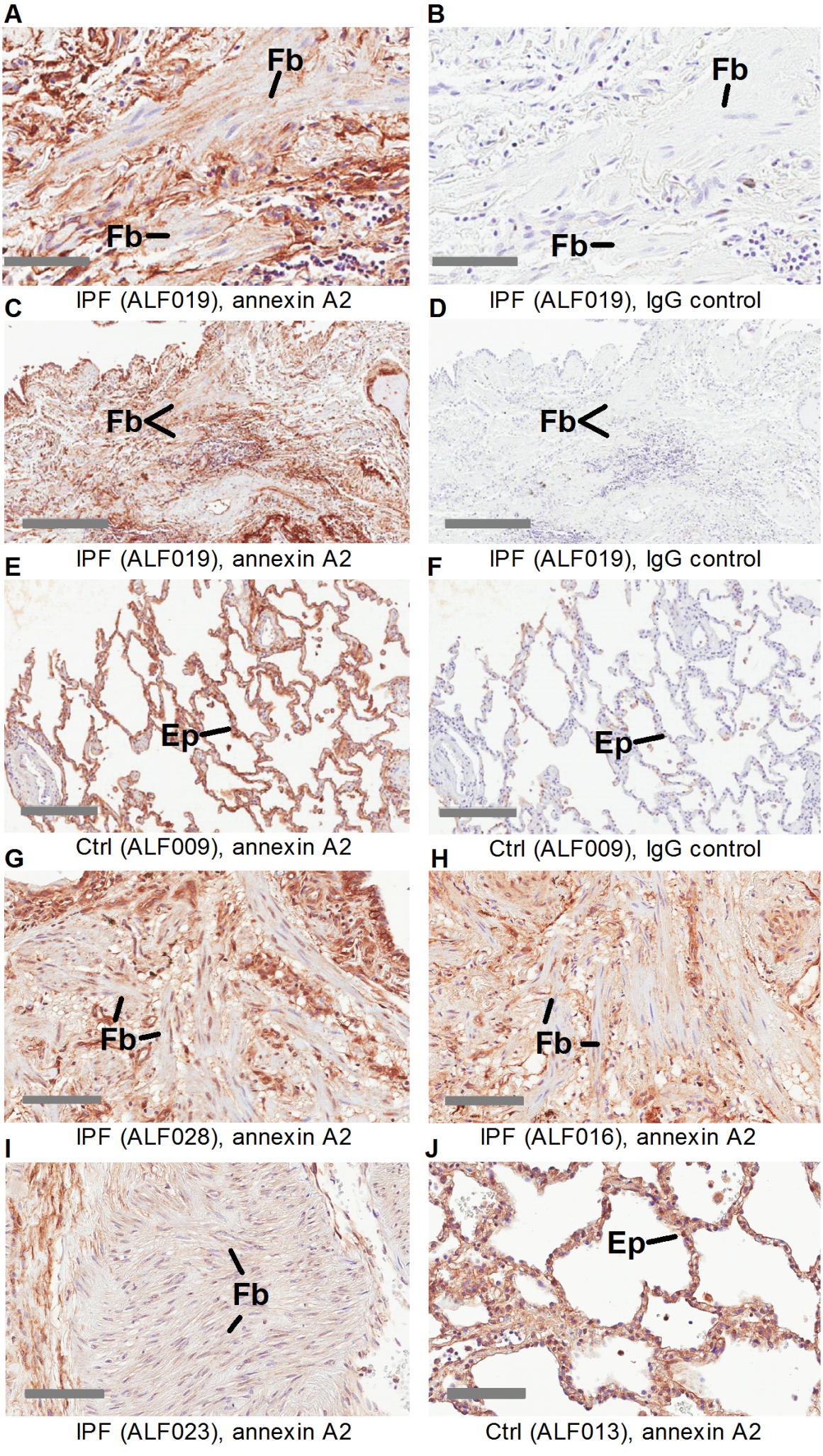
A
Fb
Fb
IPF (ALF019), annexin A2
B
Fb
Fb
IPF (ALF019), IgG control
C
Fb
IPF (ALF019), annexin A2
D
Fb
IPF (ALF019), IgG control
E
Ep
Ctrl (ALF009), annexin A2
F
Ep
Ctrl (ALF009), IgG control
G
Fb
IPF (ALF028), annexin A2
H
Fb
IPF (ALF016), annexin A2
I
Fb
IPF (ALF023), annexin A2
J
Ep
Ctrl (ALF013), annexin A2

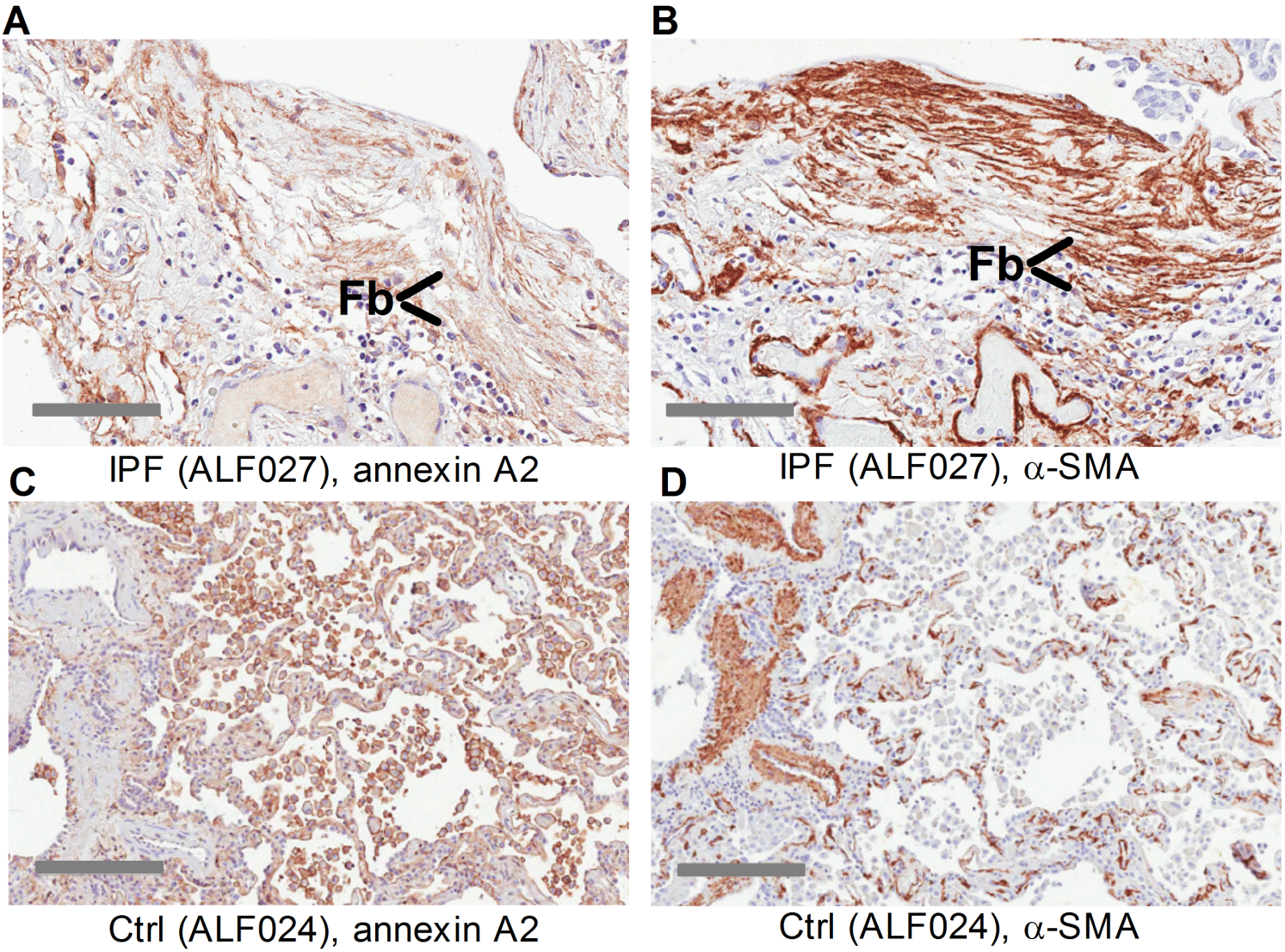
A
Fb
IPF (ALF027), annexin A2
B
Fb
IPF (ALF027), α-SMA
C
Ctrl (ALF024), annexin A2
D
Ctrl (ALF024), α-SMA

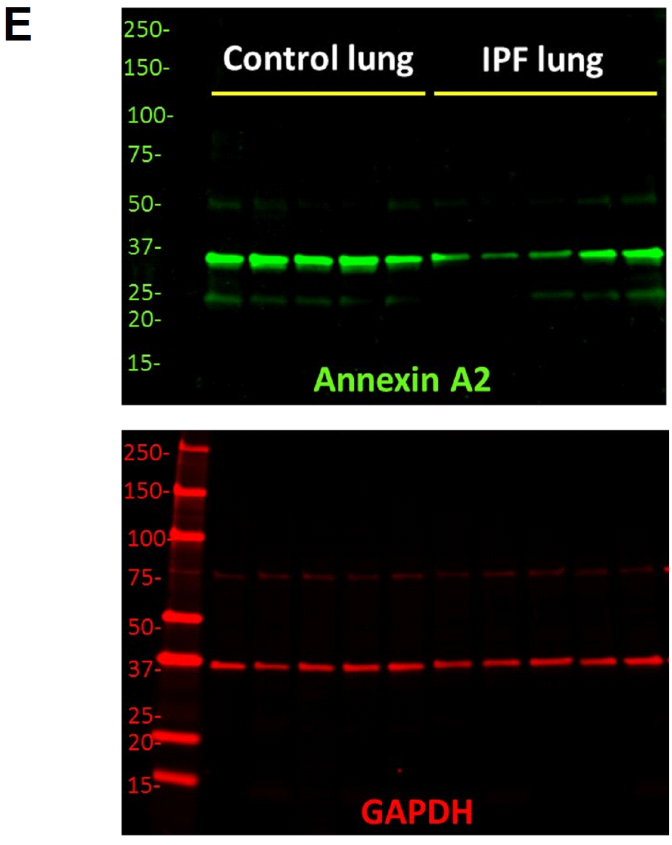
E
250-
150-
100-
75-
50-
37-
25-
20-
15-
Control lung
IPF lung
Annexin A2
250-
150-
100-
75-
50-
37-
25-
20-
15-
GAPDH

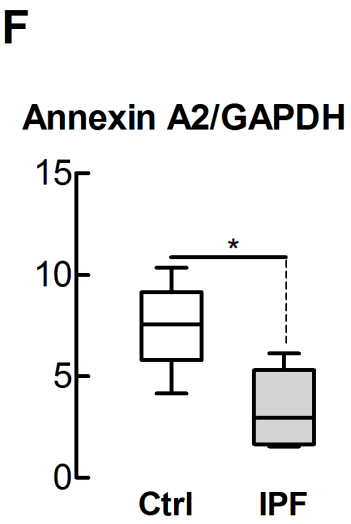
F
Annexin A2/GAPDH
15
10
5
0
*
Ctrl
IPF

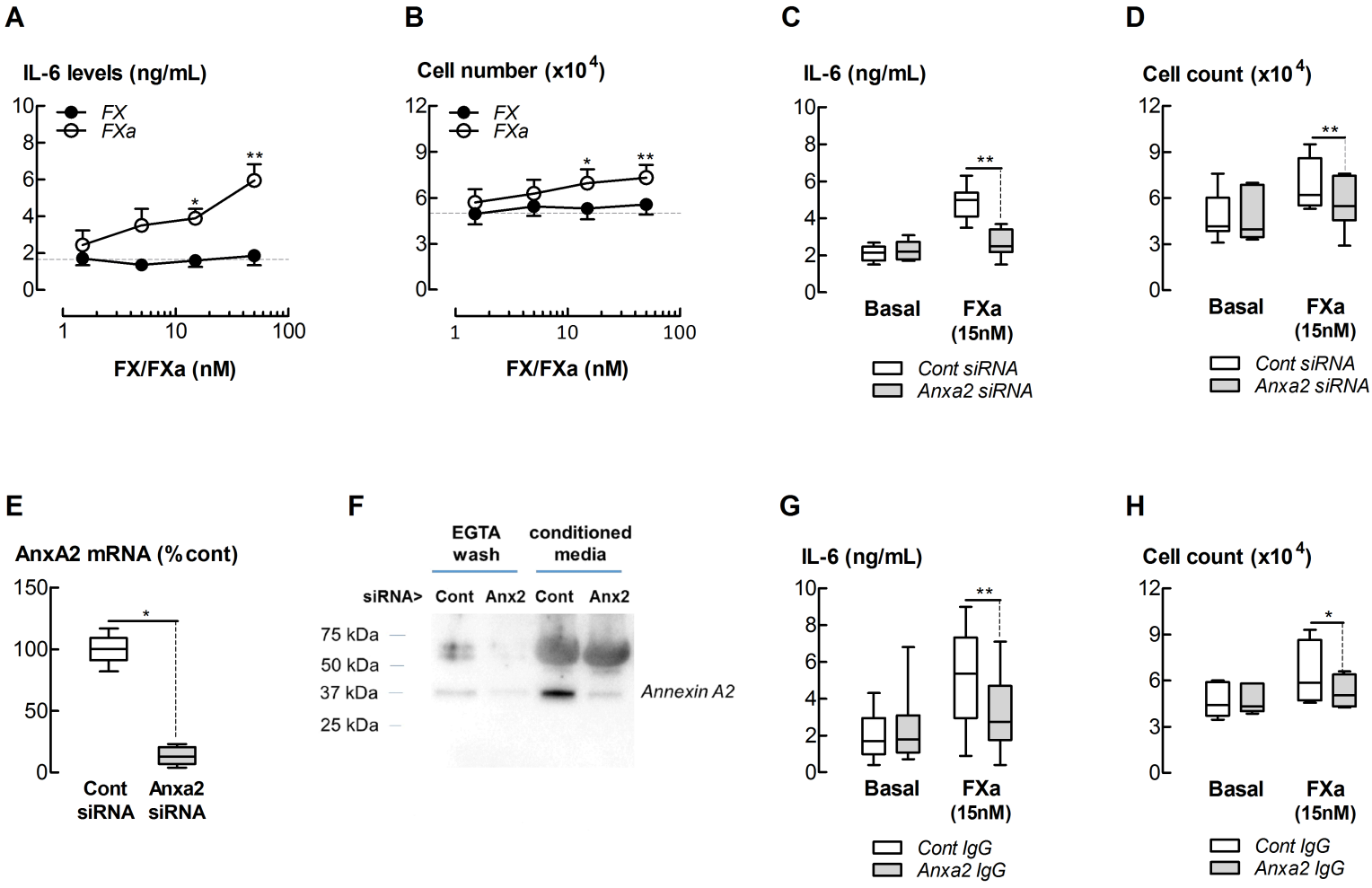
A
IL-6 levels (ng/mL)
FX
FXa
FX/FXa (nM)
B
Cell number (x10^4)
FX
FXa
FX/FXa (nM)
C
IL-6 (ng/mL)
Basal
FXa (15nM)
Cont siRNA
Anxa2 siRNA
D
Cell count (x10^4)
Basal
FXa (15nM)
Cont siRNA
Anxa2 siRNA
E
AnxA2 mRNA (%cont)
Cont siRNA
Anxa2 siRNA
F
EGTA wash
conditioned media
siRNA> Cont Anx2 Cont Anx2
75 kDa
50 kDa
37 kDa
25 kDa
Annexin A2
G
IL-6 (ng/mL)
Basal
FXa (15nM)
Cont IgG
Anxa2 IgG
H
Cell count (x10^4)
Basal
FXa (15nM)
Cont IgG
Anxa2 IgG

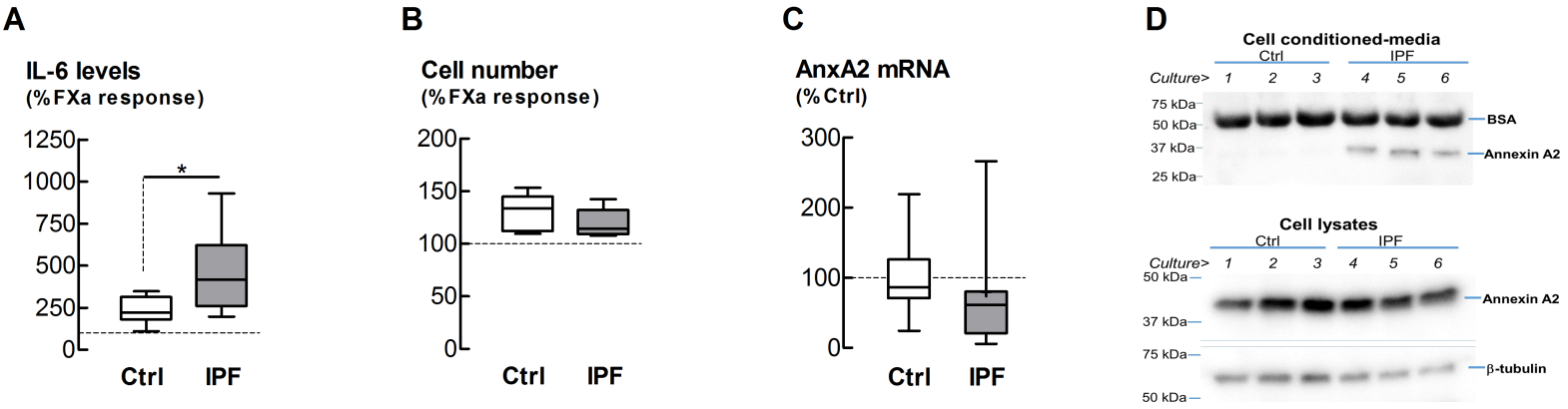
A
IL-6 levels
(%FXa response)
1250
1000
750
500
250
0
*
Ctrl
IPF
B
Cell number
(%FXa response)
200
150
100
50
0
Ctrl
IPF
C
AnxA2 mRNA
(%Ctrl)
300
200
100
0
Ctrl
IPF
D
Cell conditioned-media
Ctrl
IPF
Culture>
1
2
3
4
5
6
75 kDa
50 kDa
37 kDa
25 kDa
BSA
Annexin A2
Cell lysates
Ctrl
IPF
Culture>
1
2
3
4
5
6
50 kDa
37 kDa
75 kDa
50 kDa
Annexin A2
β-tubulin

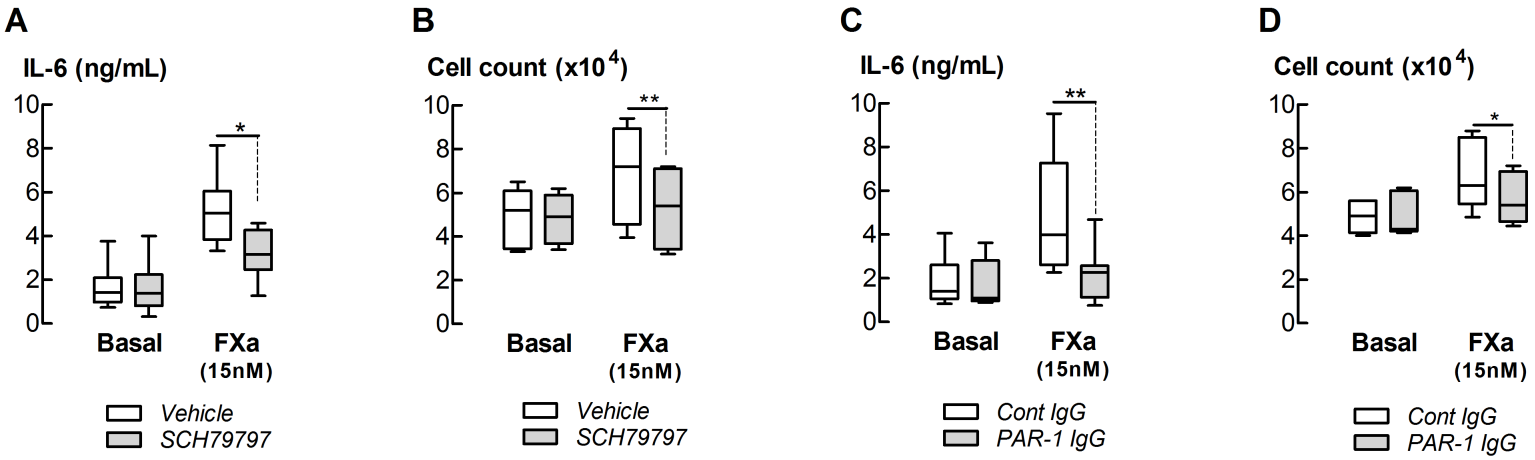
A
IL-6 (ng/mL)
10
8
6
4
2
0
*
Basal
FXa
(15nM)
Vehicle
SCH79797
B
Cell count (x10 4)
10
8
6
4
2
0
**
Basal
FXa
(15nM)
Vehicle
SCH79797
C
IL-6 (ng/mL)
10
8
6
4
2
0
**
Basal
FXa
(15nM)
Cont IgG
PAR-1 IgG
D
Cell count (x10 4)
10
8
6
4
2
0
*
Basal
FXa
(15nM)
Cont IgG
PAR-1 IgG

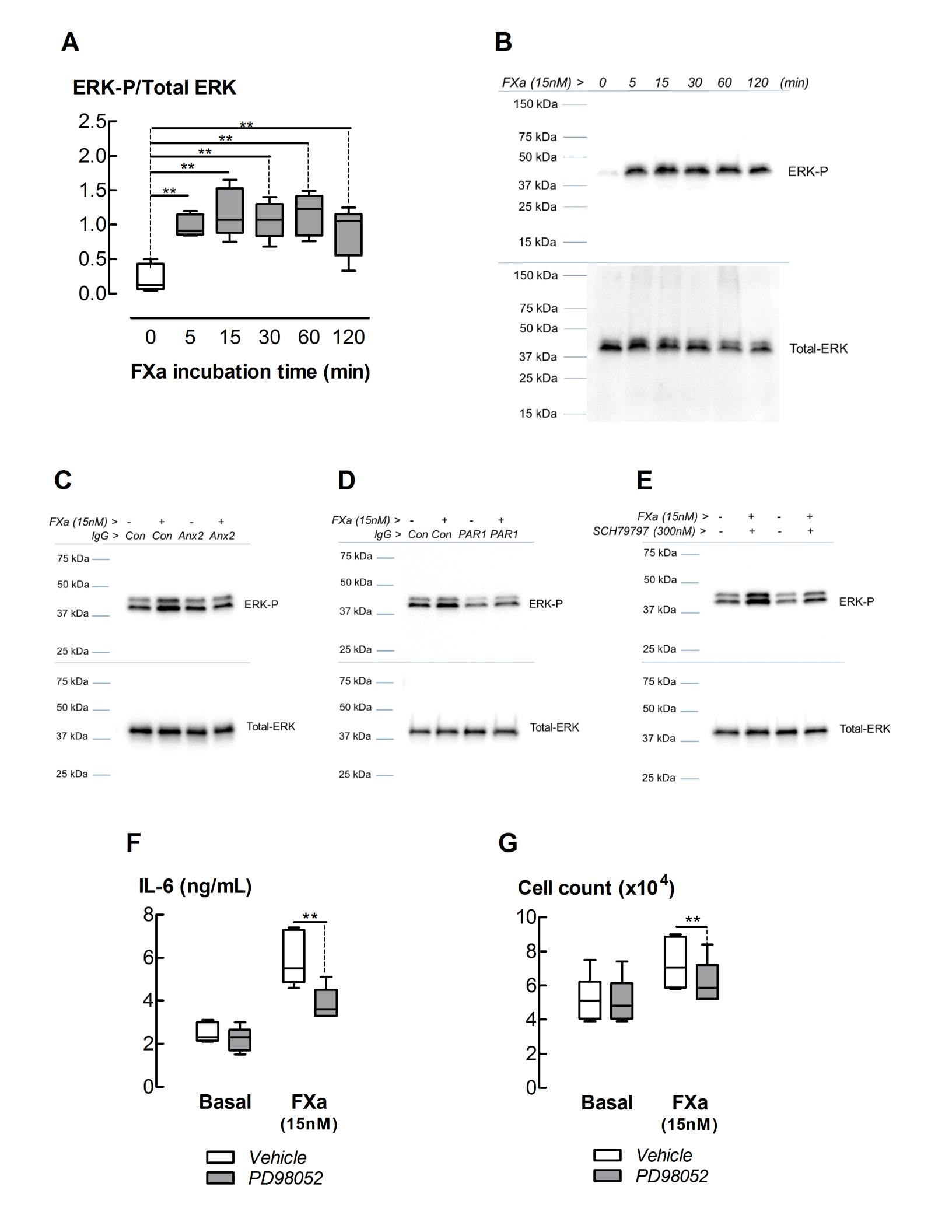
A
ERK-P/Total ERK
2.5
2.0
1.5
1.0
0.5
0.0
**
**
**
**
**
0 5 15 30 60 120
FXa incubation time (min)
B
FXa (15nM) > 0 5 15 30 60 120 (min)
150 kDa
75 kDa
50 kDa
37 kDa
25 kDa
15 kDa
ERK-P
150 kDa
75 kDa
50 kDa
37 kDa
25 kDa
15 kDa
Total-ERK
C
FXa (15nM) > - + - +
IgG > Con Con Anx2 Anx2
75 kDa
50 kDa
37 kDa
25 kDa
ERK-P
Total-ERK
D
FXa (15nM) > - + - +
IgG > Con Con PAR1 PAR1
75 kDa
50 kDa
37 kDa
25 kDa
ERK-P
Total-ERK
E
FXa (15nM) > - + - +
SCH79797 (300nM) > - + - +
75 kDa
50 kDa
37 kDa
25 kDa
ERK-P
Total-ERK
F
IL-6 (ng/mL)
8
6
4
2
0
**
Basal
FXa (15nM)
Vehicle
PD98052
G
Cell count (x10^4)
10
8
6
4
2
0
**
Basal
FXa (15nM)
Vehicle
PD98052

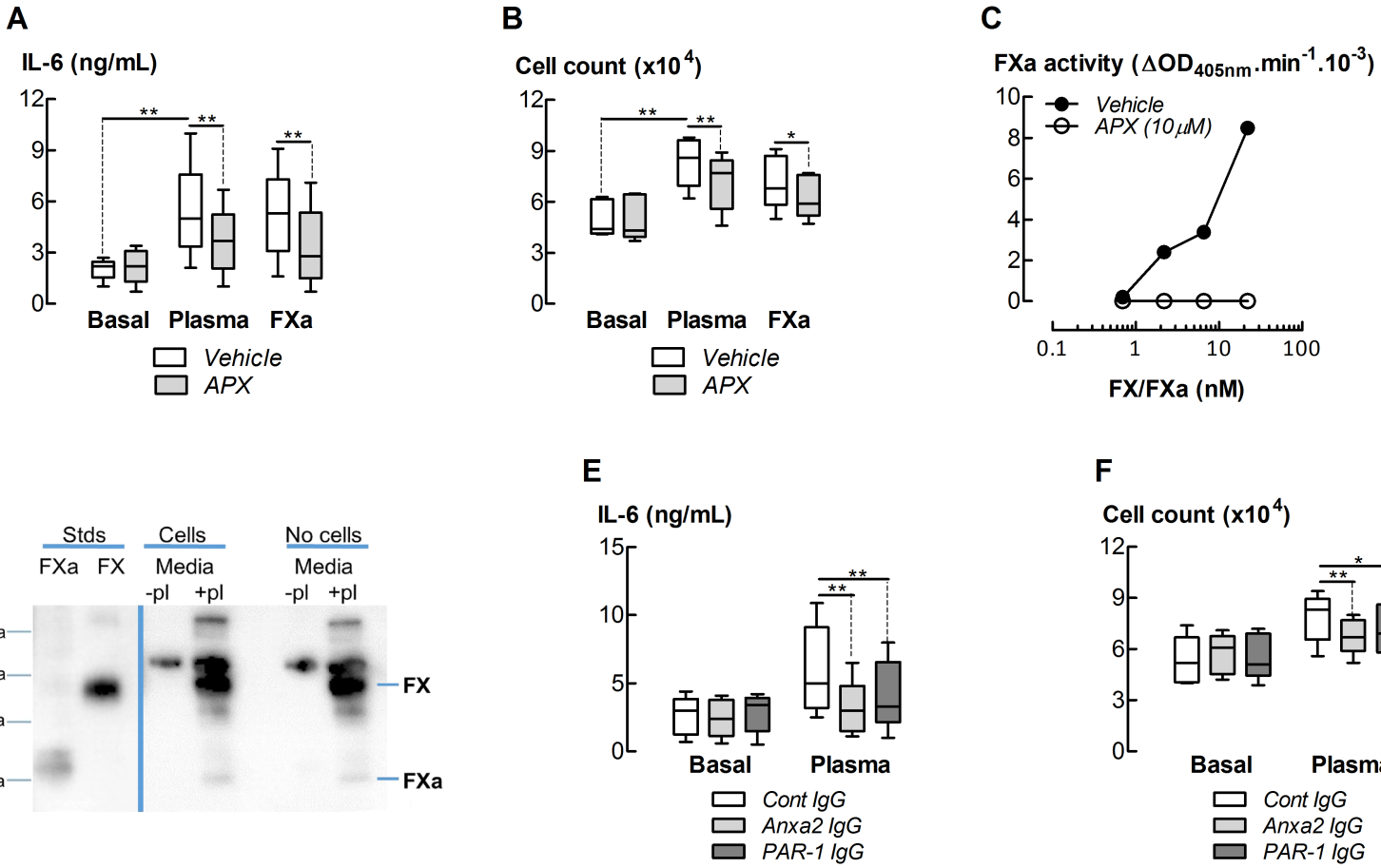
A
IL-6 (ng/mL)
12
9
6
3
0
**
**
**
Basal
Plasma
FXa
Vehicle
APX
B
Cell count (x10 4)
12
9
6
3
0
**
**
*
Basal
Plasma
FXa
Vehicle
APX
C
FXa activity (ΔOD405nm.min-1.10-3)
10
8
6
4
2
0
Vehicle
APX (10μM)
0.1
1
10
100
FX/FXa (nM)
D
Stds
Cells
No cells
FXa
FX
Media
-pl
+pl
Media
-pl
+pl
75 kDa
50 kDa
37 kDa
25 kDa
FX
FXa
E
IL-6 (ng/mL)
15
10
5
0
**
**
Basal
Plasma
Cont IgG
Anxa2 IgG
PAR-1 IgG
F
Cell count (x10 4)
12
9
6
3
0
*
**
Basal
Plasma
Cont IgG
Anxa2 IgG
PAR-1 IgG

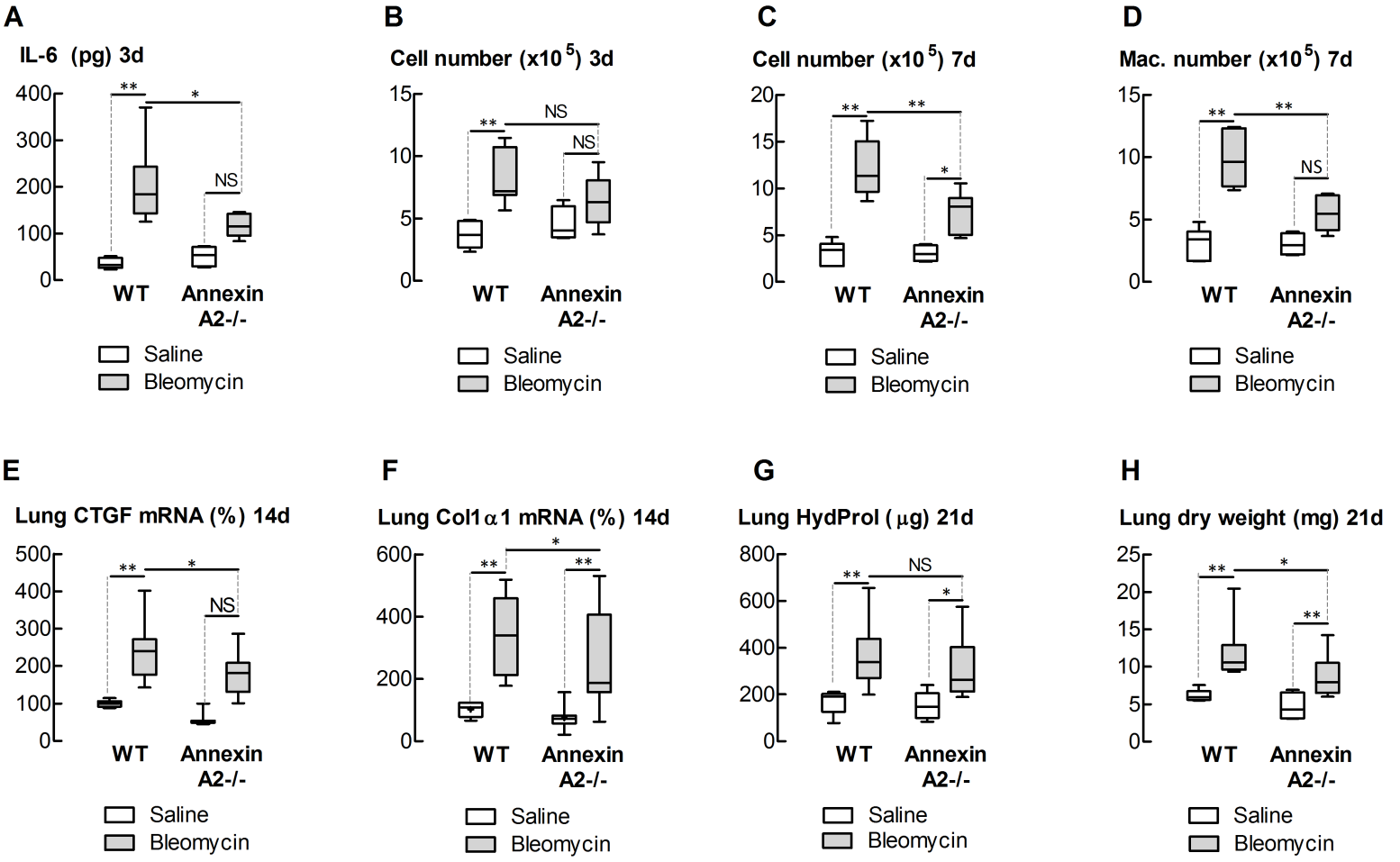
A
IL-6 (pg) 3d
400
300
200
100
0
**
*
NS
WT
Annexin A2-/-
Saline
Bleomycin
B
Cell number (x10 5) 3d
15
10
5
0
**
NS
NS
WT
Annexin A2-/-
Saline
Bleomycin
C
Cell number (x10 5) 7d
20
15
10
5
0
**
**
*
WT
Annexin A2-/-
Saline
Bleomycin
D
Mac. number (x10 5) 7d
15
10
5
0
**
**
NS
WT
Annexin A2-/-
Saline
Bleomycin
E
Lung CTGF mRNA (%) 14d
500
400
300
200
100
0
**
*
NS
WT
Annexin A2-/-
Saline
Bleomycin
F
Lung Col1α1 mRNA (%) 14d
600
400
200
0
**
*
**
WT
Annexin A2-/-
Saline
Bleomycin
G
Lung HydProl (μg) 21d
800
600
400
200
0
**
NS
*
WT
Annexin A2-/-
Saline
Bleomycin
H
Lung dry weight (mg) 21d
25
20
15
10
5
0
**
*
**
WT
Annexin A2-/-
Saline
Bleomycin